

Minireview

Insights into enzyme structure and dynamics elucidated by amide H/D exchange mass spectrometry[☆]

Laura S. Busenlehner^{a,*}, Richard N. Armstrong^{a,b}

^a Department of Biochemistry, Center in Molecular Toxicology, Vanderbilt University School of Medicine, Nashville, TN 37232-0416, United States

^b Department of Chemistry, Vanderbilt University School of Medicine, Nashville, TN 37232-0416, United States

Received 2 August 2004, and in revised form 2 September 2004

Available online 5 October 2004

Abstract

Conformational changes and protein dynamics play an important role in the catalytic efficiency of enzymes. Amide H/D exchange mass spectrometry (H/D exchange MS) is emerging as an efficient technique to study the local and global changes in protein structure and dynamics due to ligand binding, protein activation–inactivation by modification, and protein–protein interactions. By monitoring the selective exchange of hydrogen for deuterium along a peptide backbone, this sensitive technique probes protein motions and structural elements that may be relevant to allostery and function. In this report, several applications of H/D exchange MS are presented which demonstrate the unique capability of amide hydrogen/deuterium exchange mass spectrometry for examining dynamic and structural changes associated with enzyme catalysis.

© 2004 Elsevier Inc. All rights reserved.

Keywords: Hydrogen exchange; Mass spectrometry; Protein dynamics; Enzymes; Allostery

The backbone of a protein contains a unique set of tandem chemical reporters, the amide NH group. Backbone amide hydrogen/deuterium (H/D)¹ exchange is emerging as an attractive technique that has been used for over three decades to investigate protein structure and dynamics [1–6]. The kinetics of amide H/D ex-

change can be measured by several methods, however the two more commonly used techniques are nuclear magnetic resonance (NMR) spectroscopy and mass spectrometry (MS). The principal advantage of NMR spectroscopy is that amide H/D exchange rates can be determined for specific residues and hence has a high degree of spatial resolution. The limitations of NMR spectroscopy lie in its modest sensitivity and difficulties with proteins having molecular masses in excess of 50 kDa.

Driven by advances in instrumentation over the last decade, mass spectrometry has emerged as an attractive alternative to NMR [7] (for a comprehensive review see [8]). Analysis of H/D exchange kinetics by mass spectrometry (H/D exchange MS) has certain advantages in that there is no practical size limitation to the protein, the working protein concentrations can be in the sub-micromolar range, and the technique can be easily extended to membrane proteins. Spatial resolution is typically achieved by proteolysis and mass analysis of the peptide fragments [9]. However, since H/D exchange

[☆] This work was Supported by Grants F32 ES13105 (to L.S.B.), T32 ES07028 (to L.S.B., R.N.A.), P30 ES00267 (to R.N.A.), and R01 GM30910 (to R.N.A.) from the National Institutes of Health.

* Corresponding author. Fax: +1 615 343 2921.

E-mail addresses: laura.busenlehner@vanderbilt.edu (L.S. Busenlehner), r.armstrong@vanderbilt.edu (R.N. Armstrong).

¹ Abbreviations used: H/D, hydrogen/deuterium; NMR, nuclear magnetic resonance; MS, mass spectrometry; GSH, glutathione; MKK1, mitogen-activated protein kinase kinase-1; PKA, protein kinase A; HGPRT, hypoxanthine–guanine phosphoribosyltransferase; PRPP, α -D-5-phosphoribosyl 1-pyrophosphate; TM, thrombomodulin; ABE1, anion binding exosite 1; ATR-FTIR, attenuated total reflection Fourier transform infrared spectroscopy; MGST1, membrane-bound, microsomal glutathione transferase; NEM, N-ethylmaleimide; FT-ICR, Fourier transform ion cyclotron resonance.

MS yields information on short segments of the protein its structural resolution is typically not as high as can be achieved with NMR spectroscopy. This lack of site-specific information can, in principle, be resolved with the use of tandem MS/MS techniques, which can yield the same spatial resolution as the NMR method.

Amide H/D exchange mass spectrometry is a sensitive technique that can be used to study the changes in protein structure and dynamics due to protein–protein interactions, ligand binding, and protein modification, even if these changes are subtle. In addition, the technique can also be used to monitor protein folding or to determine the stability of proteins under various conditions. In this review, we present a brief survey of amide H/D exchange MS as it relates to the investigation of enzyme structure and dynamics. The practicality of H/D exchange MS to enzymology has been demonstrated for a variety of enzymes, and has been used to study local and long-range conformational changes that occur in enzymes upon substrate and cofactor binding, beyond mapping these binding sites [10–13]. In addition, H/D exchange MS has been extended to enzyme complexes with transition state analogs and inhibitors to yield valuable structural and mechanistic data [14–17]. The use of H/D exchange MS to monitor the structural effects of enzyme modification, such as phosphorylation, has also been reported [10,18–20]. Structural and mechanistic information can also be obtained with active and inactive mutant enzymes [21–23]. Topological information for enzyme–peptide and protein–protein complexes can also be attained by H/D exchange MS regardless of size, and can even yield information as to how regulatory and catalytic subunits of an enzyme interact [24–26]. These studies demonstrate the unique capability of amide hydrogen/deuterium exchange mass spectrometry for examining dynamic and structural changes associated with enzyme catalysis.

Hydrogen/deuterium exchange mass spectrometry

History

Hydrogen–deuterium exchange was first introduced through the pioneering work of Linderstrøm-Lang and colleagues in the mid-1950s, who after the discovery of protein α -helices and β -sheets, realized that amide hydrogen exchange rates should reflect the presence of hydrogen bonded structure [1,2,27]. Linderstrøm-Lang was also the first to note the relationship between the rate of hydrogen exchange and protein dynamics, and his mathematical descriptions form the basis for current exchange models. The advent of liquid scintillation technology in the 1960s spurred the use of hydrogen–tritium exchange to study native protein exchange rates [28]. Rosa and Richards [4] enhanced the spatial resolution

by combining proteolysis with newly discovered HPLC separation techniques, and Englander et al. [3] improved the technique in the early 1980s. In 1993, Zhang and Smith [9] were the first to combine hydrogen–deuterium exchange with mass spectrometry, while Johnson and Walsh [29] first reported the use of electrospray ionization in 1994. Improvements of the various steps of H/D exchange MS have been reported since the mid-1990s [10,30–32], and the technique is emerging as an essential tool to study protein structure in solution.

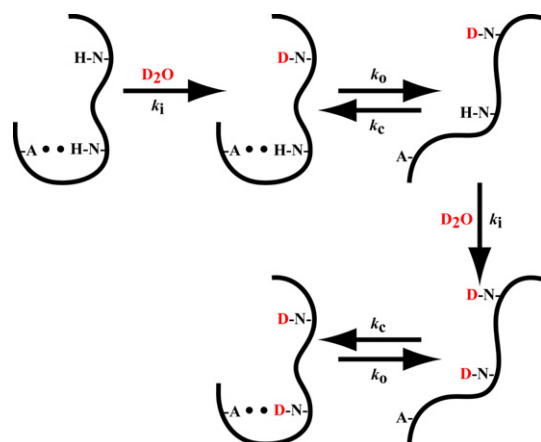
Theory

Of the many exchangeable hydrogens present in a protein, only those located on peptide amide linkages are used for H/D exchange studies. The kinetics of backbone amide H/D exchange is dependent on a variety of factors including protein structure, pH, and adjacent amino acid side-chains of the amide group [33,34]. Amide hydrogen chemical exchange with solvent can be catalyzed by acid (D_3O^+), base (OD^-), water (D_2O), or buffer solutes. At neutral pH, exchange is base-catalyzed (OD^-) by proton abstraction (for a comprehensive discussion see [35]). Despite the compact folded structure of most proteins which hinders access by the OD^- catalyst, there are some solvent exposed amide hydrogens that exchange relatively rapidly, with the average intrinsic rate of the order of $k_i \approx 10 s^{-1}$ (pH 7, 25 °C) [34]. Amide protons that are inaccessible to solvent or are participating in stable hydrogen bonds must undergo transient distortion of local structure to allow hydrogen bonding to the hydroxide ion and thus have significantly slower exchange rates, by as much as eight orders of magnitude, if they exchange at all [9,27,35]. This significant decrease in the exchange rates of amide hydrogens in a folded protein makes H/D isotopic exchange an excellent and sensitive probe for monitoring protein conformational changes and dynamic processes [8].

The rate of H/D exchange in a folded protein depends on structural fluctuations that result in “open” and “closed” conformations as illustrated in Fig. 1 [8,36]. According to the solvent penetration model, these fluctuations allow access of the OD^- catalyst, and hydrogen-bonded or buried amide hydrogens may exchange through local or global unfolding mechanisms and small-amplitude dynamic fluctuations [8,36]. Local unfolding and dynamic motions are described by equilibria between solvent-inaccessible and solvent-accessible protein states. For this mechanism, the experimental rate constant for exchange (k_{ex}) is given by Eq. (1),

$$k_{ex} = k_o k_i / (k_o + k_c + k_i), \quad (1)$$

where k_i is the intrinsic rate constant for exchange (i.e., the exchange rate constant in the fully unfolded form),



$$k_{\text{ex}} = k_0 k_i / (k_0 + k_c + k_i)$$

$$\text{EX2: } k_c \gg k_i, \quad k_{\text{ex}} = (k_0/k_c) k_i$$

$$\text{EX1: } k_i \gg k_c, \quad k_{\text{ex}} = k_0$$

Fig. 1. Linderstrom-Lang model of hydrogen exchange. Amide hydrogen exchange at neutral pH involves protein structure fluctuations that result in open and closed conformations, which are described by the kinetic rates of opening and closing, k_o and k_c , respectively. Hydrogens which are involved in hydrogen bonding or are solvent inaccessible exchange with a rate constant (k_{ex}) that is dependent on the equilibrium fluctuations between the open and closed states (k_o and k_c) as well as the intrinsic rate of exchange for an individual amide hydrogen. The equations describing the EX2 and EX1 exchange regimes are shown [1,33,36,37].

and k_o and k_c are the rate constants of opening and closing, respectively. For most stable proteins at neutral pH, the rate of closing is much faster than the rate of opening ($k_c \gg k_o$). In one amide hydrogen exchange mechanism termed EX2, or uncorrelated exchange, refolding of the locally unfolded form occurs much faster than the rate of hydrogen exchange ($k_c \gg k_i$). The rate expression can be further simplified as in Eq. (2) [36].

$$k_{\text{ex}} = k_o k_i / (k_c + k_i) = (k_o/k_c) k_i. \quad (2)$$

This rate expression for amide proton exchange depends on the rate constant for intrinsic exchange and the equilibrium constant between the open and closed states ($K_{\text{eq}} = k_o/k_c$) which embodies the molecular dynamics of the protein occurring on the microsecond to millisecond timescales [8].

In another extreme termed EX1, or correlated exchange, the rate of intrinsic amide hydrogen exchange is much faster than the rate of closing ($k_i \gg k_c$), and the rate constant for exchange is a measure of the rate of opening (k_o). The rate expression (Eq. (1)) simplifies to Eq. (3) [36,37].

$$k_{\text{ex}} = k_o. \quad (3)$$

In this exchange regime, global unfolding motions involve the simultaneous exposure of many amide hydro-

gens in a region to solvent. For unstable protein structures, whether native or induced by denaturants, the observed exchange rate is independent of the intrinsic rate of exchange for a particular amide hydrogen and is governed by exposure to solvent upon protein unfolding events. Where EX2 exchange leads to a random distribution of deuterium within a peptide, EX1 exchange yields peptides that have regions that contain either no deuterium or fully deuterated leading to a bimodal isotope pattern in the mass spectra. For these proteins, unfolding events occur on a millisecond timescale [36].

Method overview

The general procedure used to study amide H/D exchange kinetics by mass spectrometry is depicted in Fig. 2 and begins with initiating isotopic exchange of amide hydrogens (“in-exchange”) by incubating the folded protein in D_2O (pH 7, 25 °C) for a series of time points anywhere from 10 s to days, if needed. Isotopic exchange is quenched by decreasing the pH* to 2.4 and the temperature to 0 °C. Lowering both the temperature and pH results in an $\sim 10^5$ reduction in the exchange rate, thereby “trapping” the deuterium label by reducing the back-exchange of hydrogen onto the

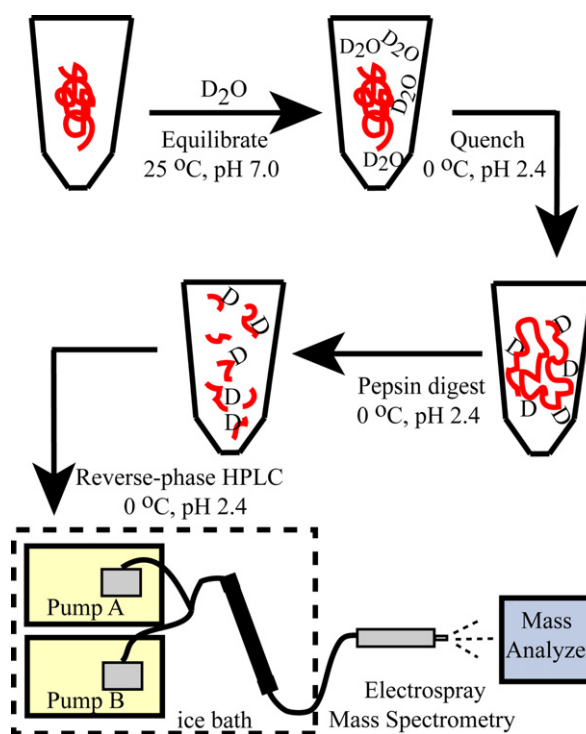


Fig. 2. Method overview of H/D exchange mass spectrometry. A native protein (pH 7.0, 25 °C) is incubated with D_2O to initiate exchange of amide hydrogens. After incubation, the exchange is quenched by lowering the pH to 2.4 and temperature to 0 °C. Pepsin is added and the resulting peptides are injected onto a reverse-phase column and separated by HPLC connected in-line to a mass spectrometer.

amide group [38]. Importantly, other exchangeable groups on the protein exhibit relatively rapid back exchange, hence the trapped isotope resides exclusively in the backbone amide groups. In addition, the low pH* mildly denatures the protein to facilitate the subsequent cleavage by pepsin, an acid-stable protease. These pepsin-generated peptide fragments, whose amino acid sequences have been confirmed by tandem MS/MS or other techniques, are separated by HPLC at 0 °C and introduced directly into a mass spectrometer usually by positive ion electrospray ionization (+ESI). The level of amide-based deuterium incorporated into each peptide can be determined by the change in molecular mass as a function of time, after correction for any in-exchange during digestion ($m_{0\%}$) and loss of the deuterium label during fractionation ($m_{100\%}$). The corrected amount of incorporated deuterium (D) calculated from the centroid of the peptide isotope mass envelope is given by Eq. (4),

$$D = \left[N \left(\frac{m_t - m_{0\%}}{m_{100\%} - m_{0\%}} \right) \right], \quad (4)$$

where N is the total number of exchangeable amide hydrogens minus any proline residues and the N-terminal amide, and where $m_{0\%}$, m_t , and $m_{100\%}$ are the average molecular masses of the same peptide in the non-deuterated, the partially deuterated at time t , and the fully-deuterated control samples, respectively [9]. The corrected amount of deuterium (D) in each peptide is then plotted versus time and fit to the sum of first-order rate terms given by Eq. (5),

$$D = N - \sum_{i=1}^N \exp(-k_i t), \quad (5)$$

where N is the number of amide protons that exchange at a given rate constant, k_i , during the time allowed for isotopic exchange, t [9]. In practice, amide hydrogen exchange rates can be divided into rapid, intermediate, and slow exchange regimes and these progress curves can be fit to between one and three exponentials depending on the complexity of the exchange process and the number of data points collected.

It is certainly possible to measure the individual rate-constant for H/D exchange of a site or groups of sites in a protein with a high degree of precision. However, one of the most informative uses of the technique is derived from the comparison of the experimental rate constant for exchange of a perturbed state, k_{ex} , to that of some reference state, $k_{\text{ex}}^{\text{ref}}$. In the EX2 exchange limit, for example, the ratio of the rate constants is a good estimate of the ratio of equilibrium constants for a conformational fluctuation. Thus changes in the exchange rates, for instance in a mutant protein, can be directly related an alteration in the equilibrium position of a conformational fluctuation (Eq. (6)) [21].

$$k_{\text{ex}}/k_{\text{ex}}^{\text{ref}} \approx (k_o/k_c)/(k_o/k_c)^{\text{ref}} = K_{\text{conf}}/K_{\text{conf}}^{\text{ref}}. \quad (6)$$

Structure and dynamics

Amide hydrogen/deuterium exchange kinetics can vary dramatically within a protein due to hydrogen bonding, solvent accessibility, and backbone flexibility [33,34]. Therefore, the amide exchange rate is highly dependent on protein structure, as well as dynamics. With respect to enzymes, the rate of amide hydrogen exchange provides essential information for understanding function and mechanism by defining the dynamic processes the enzyme undergoes, whether on a local or global scale. To understand any structure–function relationship, it is imperative to localize the regions of the enzyme that are changing. Measurements of protein dynamics are crucial to understanding enzyme function, since static protein structures are inadequate in describing the sometimes subtle, yet seemingly complex nature of enzymatic processes.

Glutathione transferase M1-1: segmental dynamics of an active site mutant

Class mu glutathione transferase rGSTM1-1 metabolizes toxic alkylating agents by catalyzing the addition of glutathione (GSH) to endogenous and xenobiotic electrophilic compounds. Each subunit of rGSTM1-1 is composed of two domains, an N-terminal GSH binding domain (domain I) and a C-terminal substrate binding domain (domain II) [39]. Previous work established that Tyr115, located in domain II, was an important residue in catalysis [40]. The subsequent crystal structure indicated that Tyr115, which was hydrogen-bonded with Ser209 near the C-terminus, could act as a physical barrier to product release from the active site [21,39]. The structure of the Y115F mutant (Fig. 3) revealed a similar structure to that of the native enzyme with minor backbone alterations near the site of mutation, as well as in the C-terminal tail due to the loss of hydrogen bonding interactions [21].

As reported by Codreanu et al. [21], H/D exchange MS of this mutant showed enhanced exchange kinetics in the regions of the enzyme that form the channel to the active site, including distal residues in the C-terminal tail, as well as in the mu loop of domain I where contact with the C-terminal tail has been disrupted (Fig. 3). It is important to note that the ~3-fold increase in k_{cat} of the Y115F mutant is very similar to the magnitude of change in k_{ex} for the peptide segments near the access channel [21,40]. These data suggest that the change in molecular dynamics in the Y115F mutant involves coupled motions affecting product release. Taken together with the structure and other biochemical evidence, not only is Tyr115

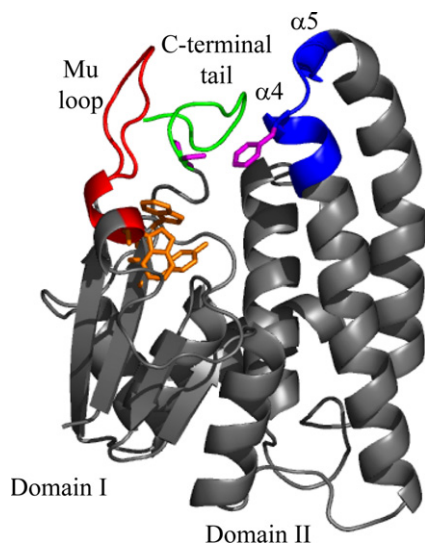


Fig. 3. The Y115F mutant of glutathione transferase M1-1. Shown in gray is the X-ray crystallographic structure of one monomer of dimeric GSTm1-1 (PDB entry 1mtc) [21]. Active site residues are in orange (Tyr6, Trp7, and Trp45). Phe115 and Ser209 are shown in magenta. Regions which show enhanced H/D exchange are as follows: mu loop (red), C-terminal tail (green), and α 4-turn- α 5 structural element harboring the Y115F mutation (blue) [21]. This figure was generated with PyMOL [114].

an important residue for function, but it also plays a structural role in catalysis by altering the release of product from the active site. Thus, amide H/D exchange kinetics by mass spectrometry can provide essential dynamic information for enzyme segmental motions that are important for catalysis, such as product release from an active site. This type of information is rarely reflected in a static X-ray crystallographic structure.

Thermophilic alcohol dehydrogenase: thermal-activated protein motions

Alcohol dehydrogenase from the thermophilic organism *Bacillus stearothermophilus* (htADH), an enzyme that catalyzes the reversible NAD^+ -dependent oxidation of alcohols to aldehydes/ketones, is known to exhibit temperature-dependent kinetic isotope effects with hydride transfer [41]. Theoretical models have predicted that the enhanced hydrogen transfer observed at higher temperatures may be due to increased protein motions, or conformational sampling, that optimize configurations for the overlap of substrate and product wave functions [41–43]. Since protein motions are a dynamic process, Liang et al. utilized amide H/D exchange MS to study whether htADH conformational flexibility was temperature dependent, and whether changes in protein mobility correlated with the rate of catalysis at elevated temperatures [44,45].

Amide hydrogen–deuterium exchange on apo-htADH was carried out between 10 and 65 °C and as ex-

pected, many peptides displayed H/D-exchange patterns where the rate of exchange increases with temperature in an Arrhenius fashion [44]. A second subset of peptides located around the substrate- and NAD^+ -binding sites exhibited discontinuous H/D-exchange behavior with a clear transition at ~ 40 °C. Weak temperature-dependence on the rate of exchange is observed below the transition temperature, whereas more significant temperature-dependence is seen above the transition temperature. Interestingly, a third subset of peptides located in the substrate-binding domain exhibits the transition at ~ 30 °C and a correlation plot of the average rate constants for H/D-exchange and k_{cat} measured at temperatures above 30 °C reveals a linear correlation between the two rates [42,45]. These results indicate that local protein motions at higher temperatures, specifically in the substrate-binding domain, enhance catalysis by populating higher-energy protein structures that result in more efficient hydride transfer.

MAP kinase kinase-1: dynamic motions accompanying activation

Mitogen-activated protein kinase kinase-1 (MKK1) is a key enzyme of the MAP kinase-signaling pathway involved in the regulation of cell growth, differentiation, and stress response [46]. As part of the cascade, MKK1 is activated by phosphorylation of Ser218 and Ser222, located within a loop as part of the conserved structural core [47,48]. Mutation of both Ser218 and Ser222 to acidic residues (S218E, S222D) along with a deletion

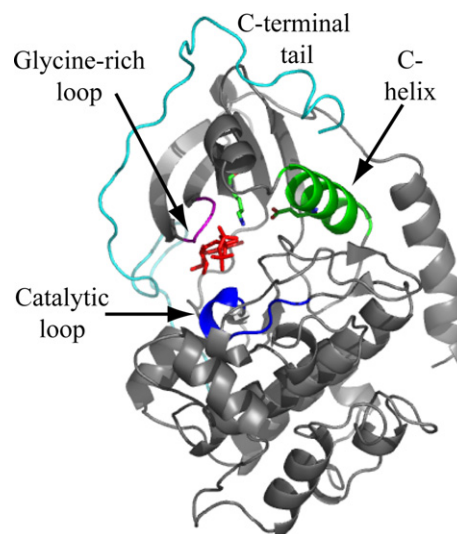


Fig. 4. The C-subunit of protein kinase A. Shown in gray is the X-ray crystallographic structure of one C-subunit of PKA (PDB entry 1atp) [62]. ATP (red) binds in the active site pocket between the two lobes of the C-subunit. The glycine-rich loop is depicted in magenta, the C-helix in green, the catalytic loop in blue, and the C-terminal tail in cyan. The conserved dyad of Lys72 and Glu91 oriented toward the ATP-binding site are indicated. This figure was generated with PyMOL [114].

of putative α -helical residues 44–51 results in a constitutively active mutant enzyme that is 530-fold more active than wild-type MKK1 [22,49,50]. Mutating the Ser residues is thought to mimic the effect of phosphorylation by enhancing the negative charge of the loop, while the deletion of 44–51 presumably disrupts structural constraints at the N-terminus [49].

Resing and Ahn addressed what role enzyme dynamics contributed to the molecular switch between inactive and active enzyme using amide H/D exchange MS [22]. The activated mutant enzyme exhibited decreased exchange rates in the proposed activation loop around the site of the mutations, attributed to the formation of new electrostatic interactions. This result is supported by structures of other protein kinases in which ionic interactions between residues in helix C and phosphorylated amino acids in the activation loop were observed [51,52]. Interestingly, within the N-terminal domain of the activated protein where other kinases are known to make several contacts with ATP [53,54], H/D exchange rates were increased. ADP release is known to be the rate limiting step of catalysis for a related kinase, therefore enhanced backbone dynamics in activated MKK1 could allow for the conformational changes upon ATP binding and ADP release [55]. These data suggest that MKK1 is activated through localized dynamic motions and increased flexibility, as well as domain closure involving the activation loop itself.

Ligand binding and protein modification

One of the most common uses for H/D exchange MS is to map unknown ligand binding sites, whether that ligand is a cofactor, substrate, inhibitor, or transition state analog, and to correlate the observed changes in enzyme dynamics to mechanism. H/D exchange MS can help to identify active sites of enzymes, especially in the absence of a high-resolution structure, and is now being used as a high-throughput screen to localize the binding sites for small molecule inhibitors [56,57]. Others use H/D exchange MS to monitor how protein modifications such as phosphorylation modulate activity of an enzyme, where modification of a single residue may lead to local and/or long-range changes in dynamics that can affect enzyme activity [10,20,58,59]. H/D exchange MS can reveal small perturbations in protein motions as a result of allostery or protein modification that many other structural techniques may not observe.

Protein kinase A: ATP-binding affects distal element to form “closed” complex

Protein kinase A (PKA) is an enzyme of the cAMP signal-transduction pathway that phosphorylates proteins involved in the pathway. The active site lies within

a pocket between two lobes of the catalytic domain (C-subunit), where ATP and a protein substrate bind (Fig. 4) [60–62]. The active site switches between the open and closed conformations by motions between the two lobes. Kinetic studies suggest that turnover is partially rate-limited by conformational changes occurring after substrate phosphorylation that have been linked, in part, to nucleotide binding and release [63–66].

To address the nature of the conformational changes that occur after phosphoryl-transfer, the ADP·C-subunit complex was subjected to H/D exchange MS by Andersen et al. [11] and compared with the apoC-subunit. Four regions of the C-subunit displayed decreased exchange in the presence of ADP. Significantly reduced exchange was localized to the conserved glycine-rich motif involved in nucleotide binding, as well as to the active site catalytic loop (Fig. 4). Part of helix-C, implicated in activation, also showed decreased exchange despite having no direct interactions with bound nucleotide [62]. In fact, these data support the hypothesis that ADP-binding may stabilize the closed state by forming a conserved electrostatic dyad (K72-E91), where K72 is known to interact with the phosphates of ATP [52,67,68]. Finally, a region of the C-terminal tail exhibited decreased exchange in the presence of ADP, consistent with this region being involved in the closed conformation and contributing to the nucleotide-binding site. H/D exchange MS provided evidence that nucleotide binding by PKA resulted in previously undefined changes in local and distal dynamics within the catalytic subunit that may reflect a portion of the rate-limiting step in catalysis.

Hypoxanthine–guanine phosphoribosyltransferase: insights into a transition-state complex

One essential enzyme for parasitic protozoan purine uptake is hypoxanthine–guanine phosphoribosyltransferase (HGPRT), which specifically catalyzes the reversible Mg^{2+} -dependent phosphoribosyl transfer from α -D-5-phosphoribosyl 1-pyrophosphate (PRPP) to hypoxanthine or guanine to form IMP or GMP, respectively. The Immucillin phosphate ImmGP, a mimic of the hypothetical GMP oxocarbenium transition state (Fig. 5A), specifically inhibits HGPRT [69,70]. The crystallographic structure of human HGPRT in complex with ImmGP and Mg^{2+} -pyrophosphate ($MgPP_i$) revealed that the transition-state analog is shielded by an antiparallel β -sheet, which was previously a disordered catalytic loop that moved ~ 25 Å to cover the active site (Fig. 5B; green) [70,71].

Wang et al. [14] used H/D exchange MS to explore the difference in solvent accessibility between three HGPRT complexes: (i) $GMP \cdot Mg$, with a partially filled active site; (ii) the internally equilibrating Michaelis complex of $IMP \cdot MgPP_i$ (94%); and (iii) the transi-

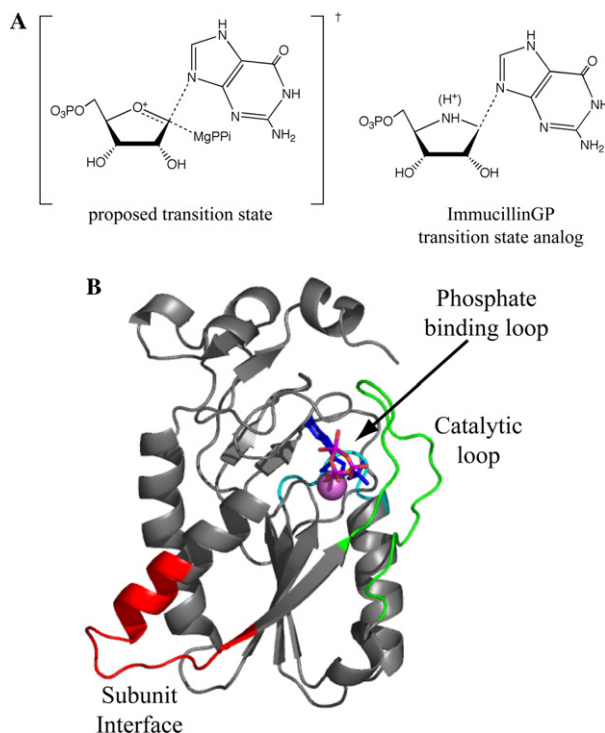


Fig. 5. HGPRT-ImmGP-MgPP_i. (A) Shown are the proposed HGPRT transition state and the transition state mimic ImmucillinGP [69]. (B) Shown in gray is the X-ray crystallographic structure of one monomer of tetrameric hypoxanthine-guanine phosphoribosyltransferase in complex with ImmucillinGP (ImmGP; blue), Mg²⁺ (purple), and pyrophosphate (PP_i; red) [70]. The structural features that undergo changes in hydrogen exchange are indicated as follows: the subunit interface (red), the catalytic loop (green), and the phosphate binding loop (cyan). This figure was generated with PyMOL [114] using PDB entry 1bzy.

tion-state analog ImmGP·MgPP_i. For the catalytic loop, both the GMP·Mg and Michaelis complexes exhibit significant H/D exchange presumably due to dynamic fluctuations. These motions are diminished upon forming the transition state complex, possibly the result of new hydrogen bonds [70,71]. Unexpectedly, a portion of the subunit interface also exhibits reduced exchange upon formation of the Michaelis complex (Fig. 5B), with additional reduction observed for the transition-state complex, and can be attributed to the before unrecognized dynamic nature of the interface. Also, bound phosphonucleotides were not sufficient to shield the phosphate-binding loop from solvent accessibility, and only the transition-state analog was able to slightly reduce exchange in this region (Fig. 5B). Given that the dissociation rate of the transition complex is too slow to explain the rapid exchange [69], the researchers suggested that the two water molecules H-bonded to phosphate oxygens become “trapped” when the catalytic loop closes, forming proton transfer bridges to local amides [70]. H/D exchange MS has provided new information of how interactions between substrate and enzyme lead to a catalytically favorable transition state.

Methylesterase CheB: phosphorylation-driven motions at the interdomain interface

CheB, a methylesterase, is involved in a bacterial chemotaxis signaling cascade pathway by specifically demethylating methylglutamate residues of other cascade proteins [72]. As a part of the pathway, CheB is activated by phosphorylation of the N-terminal regulatory domain at Asp56 (Fig. 6) [20,73]. When non-phosphorylated, the regulatory domain is proposed to act as an inhibitor by obstructing access to the active site located in the C-terminal effector domain [74]. It is thought that phosphorylation, although distant from the active site, leads to conformational changes within the interface linking the two domains [73,74]. In the absence of a structure of phosphorylated-CheB, it is unclear how phosphorylation-induced conformational changes of the regulatory domain are communicated to the effector domain.

Hughes et al. [58] employed H/D exchange MS to address how phosphorylation affects solvent accessibility at the interface between the regulatory and catalytic domains (70% phosphorylation at equilibrium). Increases in solvent accessibility were expected if phosphorylation reorients the regulatory domain allowing access to the active site. Such increases were observed in two regions of the catalytic domain containing key residues involved in domain–domain contacts (Fig. 6). However, no such increases in exchange were seen in the regulatory do-

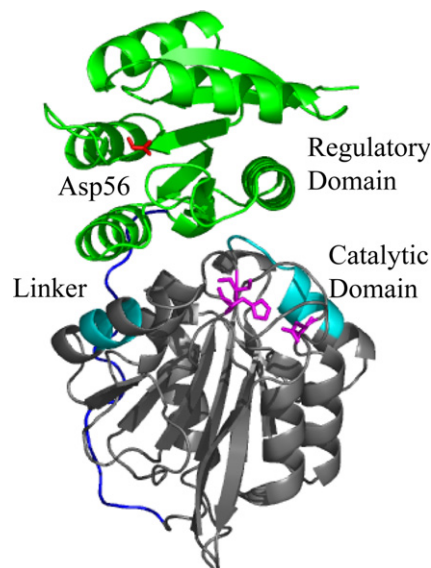


Fig. 6. CheB methylesterase. Shown is the X-ray crystallographic structure of one monomer of dimeric CheB (PDB entry 1a2o) [74]. In the catalytic domain (gray), active site residues Ser164, His190, and Asp286 are depicted in magenta. The regulatory domain is indicated in green and Asp56, the site of phosphorylation, is in red. Two peptides at the domain interface which exhibited enhanced hydrogen exchange upon phosphorylation are in shown in cyan [58]. This figure was generated with PyMOL [114].

main. Deletion of the regulatory domain of CheB indicated that the regulatory domain does protect the interfacial region of the catalytic domain from exchange, therefore the lack of changes in solvent accessibility of the regulatory domain may be due to slower motions that were unobservable over the short time course monitored (5 min). H/D exchange MS revealed that phosphorylation leads to increased solvent accessibility along the edges of the catalytic domain, however the linker region and the regulatory domain do not fully uncouple from the catalytic domain, leading to much more subtle changes than predicted based on structure alone.

Protein–protein and subunit–subunit interactions

Enzyme activation or inhibition can also be achieved by protein–protein and subunit–subunit interactions usually involving catalytic and regulatory subunits. In some cases, heteromultimeric complexes must be assembled *in vivo* for full activity. H/D exchange MS can provide insight into the solution behavior of these complexes that cannot be gleaned from three-dimensional structures. In some cases where a structure cannot be obtained, this technique can be utilized to map the interaction interfaces and even to reveal local and distal dynamic changes that affect enzyme active sites.

Protein kinase A: catalytic-regulatory subunit interactions affect distal substrate binding

PKA, introduced earlier, is composed of two regulatory (R) and two catalytic (C) subunits to form the tetrameric holoenzyme. The R-subunit is made of four domains: the dimerization/docking domain, the pseudo-substrate domain, and two tandem cAMP-binding domains (A and B) [75]. Cyclic AMP binds sequentially to the B and A domains, respectively, which leads to cooperative dissociation of the R-subunit from the C-subunit [76,77]. The primary interaction between the C- and R-subunits occurs at the cAMP-binding A domain, as well as at the pseudosubstrate region [78].

To understand how the essential residues of the regulatory subunit, R¹ α (94–224), interact with the catalytic subunit [79], H/D exchange MS was utilized by Anand et al. [80] to map these interactions and build a model of cAMP-mediated regulation of PKA activity (Fig. 7). When the C-subunit was bound to R¹ α (94–224), decreased solvent accessibility was observed for the pseudosubstrate region, a linker region not previously determined, and for specific helices (A and B) of the A domain, as well as for increased exchange within the cAMP-binding pocket. These data lead to a model where C-subunit binding to the A domain of the R-subunit induces conformational flexibility into the distal

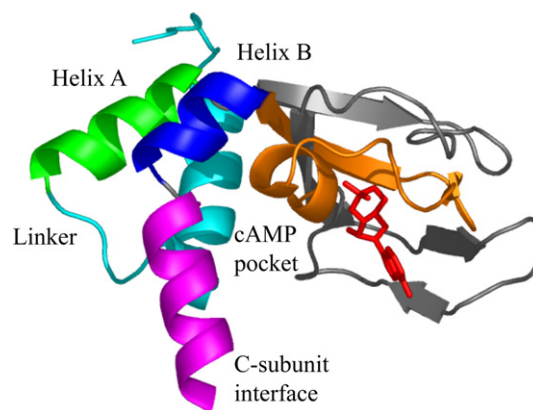


Fig. 7. The R-subunit of PKA residues 113–224. Shown in gray is one monomer of the R¹ α (113–224) subunit of protein kinase A (PDB entry 1rgs) [75]. The pseudosubstrate cAMP is shown in red. The general structural elements which exhibited altered hydrogen exchange kinetics are as follows: the linker region (cyan), helix A of cAMP-binding domain A (green), helix B of cAMP-binding domain A (blue), the C-subunit binding interface (magenta), and the cAMP-pseudosubstrate binding pocket (orange). This figure was generated with PyMOL [114].

cAMP binding pocket, and that C-subunit binding promotes release of cAMP from the R-subunit [80].

Thrombin–thrombomodulin: mapping the TM binding interface

Thrombin, a multifunctional protease, participates in the blood clotting cascade by catalyzing the proteolytic cleavage of two different substrates, fibrinogen and pro-

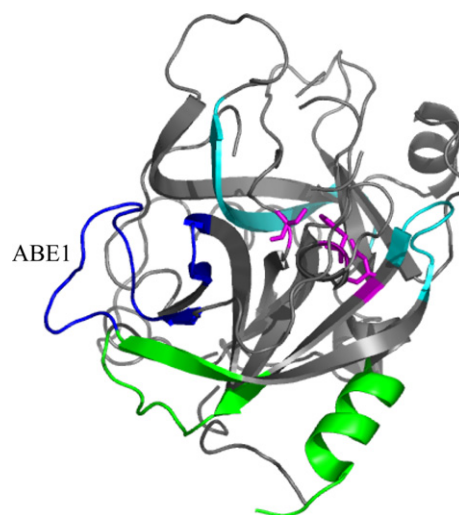


Fig. 8. Human α -Thrombin. Shown in gray is the X-ray crystallographic structure of human α -thrombin with an inhibitor (PPACK, not shown) [115]. The catalytic triad (His57, Asp102, and Ser195) of the active site is shown in magenta. Specific segments that exhibited decreases in hydrogen exchange are indicated as follows: the anion binding exosite (ABE1; blue), the tunnel to the active site (green), and the residues flanking the active site (cyan). This figure was generated with PyMOL [114] using PDB entry 1 ppb.

domain by *N*-ethylmaleimide (NEM) enhances the rate of this conformational transition and serves to activate the protein [99,100]. Two separate three-dimensional maps, calculated to a resolution of 6 Å from two-dimensional crystals, are consistent with each subunit consisting of a membrane-spanning four-helix bundle where the only difference in the structures is a change in inclination of the helices [101–103]. It is likely that the difference in the observed helix angles represents an inherent flexibility of MGST1 and may be indicative of the conformational transition required to form the enzyme–thiolate complex.

H/D exchange MS can reveal the nature of the conformational transition upon GSH binding and ionization, as well as identify the mechanism by which NEM-modification activates an MGST1-detergent complex. Busenlehner et al. [10] reported significant decreases in the exchange kinetics of the cytosolic segments that occur upon GSH binding and are consistent with extensive re-ordering of this domain (Fig. 9A). In addition, two peptides in the interior of helices 1 and 3 show an increase in exchange, likely representative of the cooperative conformational transition which involves reorientation of the transmembrane helices (Fig. 9B). NEM-alkylation of Cys49 in the cytosolic domain results in decreased exchange near the site of modification, but also leads to the same increases in exchange within helices 1 and 3. Thus, NEM-alkylation pre-organizes the helices to facilitate the conformational transition required for GSH binding and ionization, resulting in activation. The H/D exchange MS method was also extended to catalytically active, two-dimensional crystals of an MGST1–phospholipid complex in the presence of GSH to confirm that the conformational changes observed reflected the behavior of the protein in a membrane. This study indicated that the stress-sensor Cys49 acts as a molecular switch which re-orientates at least two transmembrane helices into a more favorable conformation for GSH binding and ionization.

Future directions of amide H/D mass spectrometry

Site-specific H/D exchange MS using tandem mass spectrometry

One of the main limitations of H/D exchange MS is the amount of spatial, and therefore structural, resolution that can be obtained. Pepsin cleavage results in many peptides that may cover an entire protein sequence and if some peptides overlap in a specific way, manual subtraction of the kinetic data can lead to increased spatial resolution. However, unit resolution is not possible for most proteins using this method. Many researchers have turned to site-specific H/D ex-

change MS, which utilizes tandem-MS techniques (MS/MS) to further fragment peptide ions in the gas phase into daughter ions leading to deuteration kinetics of individual amides. Although scrambling of the deuterium along the backbone during collision-induced dissociation may be problematic [29,93], many researchers have found that specific daughter ions of model peptides gave more reliable exchange data [30,92–94]. The utility of site-specific H/D exchange MS rivals that of NMR methods, but can be applied to proteins that may not be amenable to NMR spectroscopy. So far, site-specific H/D exchange MS has been applied to a few small proteins including insulin [104], viral fusion peptide [105], thioredoxin [106], cytochrome *c* [30], and model transmembrane peptides [92,94]. One of the more recent advances to the technique interfaces Fourier transform ion cyclotron resonance (FT-ICR) with MS to study protein structure [107,108] with increased sensitivity and mass accuracy.

H/D exchange MS on large multimeric complexes

H/D exchange MS is also particularly well suited to study large multi-subunit proteins and macromolecular complexes. Since the H/D exchange MS method employs a digestion step after pulse labeling with deuterium, the size and complexity of the protein become less of an issue. The combination of pepsin and other acid proteases, whether used individually as complementary experiments or together in a protease “cocktail,” may also increase spatial resolution [32]. Other physical techniques such as NMR spectroscopy have size limitations that H/D exchange MS theoretically does not have. Currently, large homo-oligomeric complexes such as rabbit muscle aldolase (157 kDa tetramer), acetohydroxy acid isomeroreductase (114 kDa dimer), and retinoid X receptor (92 kDa dimer) have been amenable to this technique [13,109,110]. Heterologous complexes have been less extensively studied using H/D exchange MS with the full complex, however H/D exchange data have been acquired on individual subunits of the F1-ATPase supramolecular complex and on truncated subunits of protein kinase A (~100 kDa complex) [80,111]. H/D exchange MS appears poised to make a significant contribution to the study of structure and dynamics of these important biological complexes.

H/D exchange MS in the millisecond time domain

Practically, measuring exchange rates for some amide protons by H/D exchange MS is limited to the inherent “hands on” nature of the experiment. In most cases, the shortest incubation time that can be performed with manual mixing is usually around 10 s. Therefore, additional exchange information is lost for those amide link-

ages that exchange far too fast to be followed by manual mixing techniques. Many of these amide protons may be reside in loops or unstructured regions that may be important for enzyme catalysis, for example the mu loop in rGSTM1-1 or the catalytic loop for HGPRT discussed previously [14,21].

Pulse-labeling with deuterium can be extended into the millisecond time domain with easily modified rapid-quench techniques and has been demonstrated for cytochrome *c* by Dharmasiri and Smith [112] and for apomyoglobin by Tsui et al. [113]. Given that the half-life for intrinsic exchange of a typical amide proton at pH 7 and 25 °C is approximately 70 ms [33], exchange at or near the intrinsic rates can be measured with this technique. H/D exchange MS using a rapid quench apparatus may also include an on-line immobilized pepsin column prior to LC/MS, which is currently utilized by several researchers [31]. Amide exchange rates of these rapidly exchanging protons can yield much more structural information about the solvent accessibility of particular amides that may be catalytically important.

Conclusions

Although many techniques provide structural information that is indispensable for enzymology, one must not overlook the importance of protein dynamics to catalysis. H/D exchange mass spectrometry has made significant contributions to the understanding of the role dynamics plays in enzyme-catalyzed reactions. The practicality of the method lies in the fact that amide hydrogens are sensitive probes of protein secondary structure, solvent accessibility, and protein motions. The recent advances in mass spectrometry allow site-specific information to be gleaned from amide H/D exchange experiments, and now H/D exchange MS is emerging as an attractive alternative to other structural techniques due to the exceptional capability of examining both dynamic and structural changes.

References

- [1] S.W. Englander, L. Mayne, Y. Bai, T.R. Sosnick, *Protein Sci.* 5 (1997) 1101–1109.
- [2] A. Hvidt, K. Linderstrom-Lang, *Biochim. Biophys. Acta* 4 (1954) 574–575.
- [3] J.J. Englander, J.R. Rogero, S.W. Englander, *Anal. Biochem.* 1 (1985) 234–244.
- [4] J.J. Rosa, F.M. Richards, *J. Mol. Biol.* 3 (1979) 399–416.
- [5] G. Thevenon-Emeric, J. Kozlowski, Z. Zhang, D.L. Smith, *Anal. Chem.* 20 (1992) 2456–2458.
- [6] G. Wagner, K. Wuthrich, *J. Mol. Biol.* 2 (1982) 343–361.
- [7] I.A. Kaltashov, S.J. Eyles, *J. Mass. Spectrom.* 6 (2002) 557–565.
- [8] A.N. Hoofnagle, K.A. Resing, N.G. Ahn, *Annu. Rev. Biophys. Biomol. Struct.* 32 (2003) 1–25.
- [9] Z. Zhang, D.L. Smith, *Protein Sci.* 4 (1993) 522–531.
- [10] L.S. Busenlehner, S.G. Codreanu, P.J. Holm, P. Bhakat, H. Hebert, R. Morgenstern, R.N. Armstrong, *Biochemistry* 43 (2004) 11145–11152.
- [11] M.D. Andersen, J. Shaffer, P.A. Jennings, J.A. Adams, *J. Biol. Chem.* 17 (2001) 14204–14211.
- [12] C. Ceccarelli, Z.X. Liang, M. Strickler, G. Prehna, B.M. Goldstein, J.P. Klinman, B.J. Bahnsen, *Biochemistry* 18 (2004) 5266–5277.
- [13] F. Halgand, R. Dumas, V. Biou, J.P. Andrieu, K. Thomazeau, J. Gagnon, R. Douce, E. Forest, *Biochemistry* 19 (1999) 6025–6034.
- [14] F. Wang, W. Shi, E. Nieves, R.H. Angeletti, V.L. Schramm, C. Grubmeyer, *Biochemistry* 27 (2001) 8043–8054.
- [15] F. Wang, R.W. Miles, G. Kicska, E. Nieves, V.L. Schramm, R.H. Angeletti, *Protein Sci.* 9 (2000) 1660–1668.
- [16] X.L. Guo, K. Shen, F. Wang, D.S. Lawrence, Z.Y. Zhang, *J. Biol. Chem.* 43 (2002) 41014–41022.
- [17] H. Mazon, O. Marcillat, E. Forest, C. Vial, *Biochemistry* 46 (2003) 13596–13604.
- [18] M.Y. Kim, C.S. Maier, D.J. Reed, P.S. Ho, M.L. Deinzer, *Biochemistry* 48 (2001) 14413–14421.
- [19] A.N. Hoofnagle, J.W. Stoner, T. Lee, S.S. Eaton, N.G. Ahn, *Biophys. J.* 1 (Pt. 1) (2004) 395–403.
- [20] G.S. Anand, P.N. Goudreau, A.M. Stock, *Biochemistry* 40 (1998) 14038–14047.
- [21] S.G. Codreanu, J.E. Ladner, G. Xiao, N.V. Stourman, D.L. Hachey, G.L. Gilliland, R.N. Armstrong, *Biochemistry* 51 (2002) 15161–15172.
- [22] K.A. Resing, N.G. Ahn, *Biochemistry* 2 (1998) 463–475.
- [23] K.M. Zawadzki, Y. Hamuro, J.S. Kim, S. Garrod, D.D. Stranz, S.S. Taylor, V.L. Woods Jr., *Protein Sci.* 9 (2003) 1980–1990.
- [24] G.S. Anand, D. Law, J.G. Mandell, A.N. Snead, I. Tsigelny, S.S. Taylor, L.F. Ten Eyck, E.A. Komives, *Proc. Natl. Acad. Sci. USA* 23 (2003) 13264–13269.
- [25] J.G. Mandell, A. Baerga-Ortiz, S. Akashi, K. Takio, E.A. Komives, *J. Mol. Biol.* 3 (2001) 575–589.
- [26] J.R. Engen, W.H. Gmeiner, T.E. Smithgall, D.L. Smith, *Biochemistry* 28 (1999) 8926–8935.
- [27] A. Hvidt, K. Linderstrom-Lang, *Biochim. Biophys. Acta* 1 (1955) 168–169.
- [28] S.W. Englander, J.J. Englander, *Methods Enzymol.* (1972) 406–413.
- [29] R.S. Johnson, K.A. Walsh, *Protein Sci.* 12 (1994) 2411–2418.
- [30] Y. Deng, H. Pan, D.L. Smith, *J. Am. Chem. Soc.* (1999) 1966–1967.
- [31] L. Wang, H. Pan, D.L. Smith, *Mol. Cell. Proteomics* 2 (2002) 132–138.
- [32] L. Cravello, D. Lascoux, E. Forest, *Rapid Commun. Mass Spectrom.* 21 (2003) 2387–2393.
- [33] R.S. Molday, S.W. Englander, R.G. Kallen, *Biochemistry* 2 (1972) 150–158.
- [34] Y. Bai, J.S. Milne, L. Mayne, S.W. Englander, *Proteins* 1 (1993) 75–86.
- [35] H. Maity, W.K. Lim, J.N. Rumbley, S.W. Englander, *Protein Sci.* 12 (2003) 153–160.
- [36] S.W. Englander, N.R. Kallenbach, *Q. Rev. Biophys.* (1984) 521–555.
- [37] H. Roder, G. Wagner, K. Wuthrich, *Biochemistry* 25 (1985) 7396–7407.
- [38] S.W. Englander, A. Poulsen, *Biopolymers* (1969) 379–393.
- [39] X. Ji, P. Zhang, R.N. Armstrong, G.L. Gilliland, *Biochemistry* 42 (1992) 10169–10184.
- [40] W.W. Johnson, S. Liu, X. Ji, G.L. Gilliland, R.N. Armstrong, *J. Biol. Chem.* 16 (1993) 11508–11511.

- [41] A. Kohen, R. Cannio, S. Bartolucci, J.P. Klinman, *Nature* 6735 (1999) 496–499.
- [42] S. Hammes-Schiffer, *Biochemistry* 45 (2002) 13335–13343.
- [43] S. Caratzoulas, J.S. Mincer, S.D. Schwartz, *J. Am. Chem. Soc.* 13 (2002) 3270–3276.
- [44] Z.X. Liang, T. Lee, K.A. Resing, N.G. Ahn, J.P. Klinman, *Proc. Natl. Acad. Sci. USA* 26 (2004) 9556–9561.
- [45] M.J. Knapp, J.P. Klinman, *Eur. J. Biochem.* 13 (2002) 3113–3121.
- [46] R. Seger, E.G. Krebs, *FASEB J.* 9 (1995) 726–735.
- [47] D.R. Alessi, Y. Saito, D.G. Campbell, P. Cohen, G. Sithanandam, U. Rapp, A. Ashworth, C.J. Marshall, S. Cowley, *EMBO J.* 7 (1994) 1610–1619.
- [48] C.F. Zheng, K.L. Guan, *EMBO J.* 5 (1994) 1123–1131.
- [49] S.J. Mansour, J.M. Candia, J.E. Matsuura, M.C. Manning, N.G. Ahn, *Biochemistry* 48 (1996) 15529–15536.
- [50] S.J. Mansour, W.T. Matten, A.S. Hermann, J.M. Candia, S. Rong, K. Fukasawa, G.F. Vande Woude, N.G. Ahn, *Science* 5174 (1994) 966–970.
- [51] L.N. Johnson, M.E. Noble, D.J. Owen, *Cell* 2 (1996) 149–158.
- [52] P.D. Jeffrey, A.A. Russo, K. Polyak, E. Gibbs, J. Hurwitz, J. Massague, N.P. Pavletich, *Nature* 6538 (1995) 313–320.
- [53] S.S. Taylor, E. Radzio-Andzelm, *Structure* 5 (1994) 345–355.
- [54] D. Bossemeyer, *Trends Biochem. Sci.* 5 (1994) 201–205.
- [55] J.A. Adams, S.S. Taylor, *Biochemistry* 36 (1992) 8516–8522.
- [56] V.L. Woods Jr., Y. Hamuro, *J. Cell. Biochem. (Suppl.)* (2001) 89–98.
- [57] R.A. Garcia, D. Pantazatos, F.J. Villarreal, *Assay Drug Dev. Technol.* 1 (2004) 81–91.
- [58] C.A. Hughes, J.G. Mandell, G.S. Anand, A.M. Stock, E.A. Komives, *J. Mol. Biol.* 4 (2001) 967–976.
- [59] A.N. Hoofnagle, K.A. Resing, E.J. Goldsmith, N.G. Ahn, *Proc. Natl. Acad. Sci. USA* 3 (2001) 956–961.
- [60] D.R. Knighton, J.H. Zheng, L.F. Ten Eyck, V.A. Ashford, N.H. Xuong, S.S. Taylor, J.M. Sowadski, *Science* 5018 (1991) 407–414.
- [61] D.R. Knighton, J.H. Zheng, L.F. Ten Eyck, N.H. Xuong, S.S. Taylor, J.M. Sowadski, *Science* 5018 (1991) 414–420.
- [62] J. Zheng, D.R. Knighton, N.H. Xuong, S.S. Taylor, J.M. Sowadski, L.F. Ten Eyck, *Protein Sci.* 10 (1993) 1559–1573.
- [63] J. Lew, S.S. Taylor, J.A. Adams, *Biochemistry* 22 (1997) 6717–6724.
- [64] Q. Ni, J. Shaffer, J.A. Adams, *Protein Sci.* 9 (2000) 1818–1827.
- [65] J. Shaffer, J.A. Adams, *Biochemistry* 37 (1999) 12072–12079.
- [66] J. Shaffer, J.A. Adams, *Biochemistry* 17 (1999) 5572–5581.
- [67] A.A. Russo, P.D. Jeffrey, N.P. Pavletich, *Nat. Struct. Biol.* 8 (1996) 696–700.
- [68] B.J. Canagarajah, A. Khokhlatchev, M.H. Cobb, E.J. Goldsmith, *Cell* 5 (1997) 859–869.
- [69] C.M. Li, P.C. Tyler, R.H. Furneaux, G. Kicska, Y. Xu, C. Grubmeyer, M.E. Girvin, V.L. Schramm, *Nat. Struct. Biol.* 6 (1999) 582–587.
- [70] W. Shi, C.M. Li, P.C. Tyler, R.H. Furneaux, C. Grubmeyer, V.L. Schramm, S.C. Almo, *Nat. Struct. Biol.* 6 (1999) 588–593.
- [71] J.C. Eads, G. Scapin, Y. Xu, C. Grubmeyer, J.C. Sacchettini, *Cell* 2 (1994) 325–334.
- [72] S.A. Simms, M.G. Keane, J. Stock, *J. Biol. Chem.* 18 (1985) 10161–10168.
- [73] G.S. Anand, P.N. Goudreau, J.K. Lewis, A.M. Stoc, *Protein Sci.* 5 (2000) 898–906.
- [74] S. Djordjevic, P.N. Goudreau, Q. Xu, A.M. Stock, A.H. West, *Proc. Natl. Acad. Sci. USA* 4 (1998) 1381–1386.
- [75] Y. Su, W.R. Dostmann, F.W. Herberg, K. Durick, N.H. Xuong, L. Ten Eyck, S.S. Taylor, K.I. Varughese, *Science* 5225 (1995) 807–813.
- [76] D.A. Johnson, P. Akamine, E. Radzio-Andzelm, M. Madhusudan, S.S. Taylor, *Chem. Rev.* 8 (2001) 2243–2270.
- [77] D. Ogreid, S.O. Doskeland, *FEBS Lett.* 2 (1981) 287–292.
- [78] R.M. Gibson, Y. Ji-Buechler, S.S. Taylor, *J. Biol. Chem.* 26 (1997) 16343–16350.
- [79] L.J. Huang, S.S. Taylor, *J. Biol. Chem.* 41 (1998) 26739–26746.
- [80] G.S. Anand, C.A. Hughes, J.M. Jones, S.S. Taylor, E.A. Komives, *J. Mol. Biol.* 2 (2002) 377–386.
- [81] E.W. Davie, K. Fujikawa, W. Kisiel, *Biochemistry* 43 (1991) 10363–10370.
- [82] C.T. Esmon, *Biochim. Biophys. Acta* 1–2 (2000) 349–360.
- [83] C.T. Esmon, *FASEB J.* 10 (1995) 946–955.
- [84] T. Myles, F.C. Church, H.C. Whinna, D. Monard, S.R. Stone, *J. Biol. Chem.* 47 (1998) 31203–31208.
- [85] R.Q. Monteiro, J.G. Raposo, A. Wisner, J.A. Guimaraes, C. Bon, R.B. Zingali, *Biochem. Biophys. Res. Commun.* 3 (1999) 819–822.
- [86] P. Fuentes-Prior, Y. Iwanaga, R. Huber, R. Pagila, G. Rumennik, M. Seto, J. Morser, D.R. Light, W. Bode, *Nature* 6777 (2000) 518–525.
- [87] C.H. Croy, J.R. Koeppe, S. Bergqvist, E.A. Komives, *Biochemistry* 18 (2004) 5246–5255.
- [88] C. Vigano, M. Smeyers, V. Raussens, F. Scheirlinckx, J.M. Ruysschaert, E. Goormaghtigh, *Biopolymers* 1–2 (2004) 19–26.
- [89] C. Tian, P.F. Gao, L.H. Pinto, R.A. Lamb, T.A. Cross, *Protein Sci.* 11 (2003) 2597–2605.
- [90] G. Veglia, A.C. Zeri, C. Ma, S.J. Opella, *Biophys. J.* 4 (2002) 2176–2183.
- [91] M.R. de Planque, B.B. Bonev, J.A. Demmers, D.V. Greathouse, R.E. Koeppe II, F. Separovic, A. Watts, J.A. Killian, *Biochemistry* 18 (2003) 5341–5348.
- [92] J.A. Demmers, J. Haverkamp, A.J. Heck, R.E. Koeppe II, J.A. Killian, *Proc. Natl. Acad. Sci. USA* 7 (2000) 3189–3194.
- [93] J.A. Demmers, D.T. Rijkers, J. Haverkamp, J.A. Killian, A.J. Heck, *J. Am. Chem. Soc.* 37 (2002) 11191–11198.
- [94] J.A. Demmers, E. van Duijn, J. Haverkamp, D.V. Greathouse, R.E. Koeppe II, A.J. Heck, J.A. Killian, *J. Biol. Chem.* 37 (2001) 34501–34508.
- [95] R.K. Hansen, R.W. Broadhurst, P.C. Skelton, I.T. Arkin, *J. Am. Soc. Mass Spectrom.* 12 (2002) 1376–1387.
- [96] T.H. Sun, R. Morgenstern, *Biochem. J.* (1997) 193–196.
- [97] C. Andersson, E. Mosialou, R. Weinander, R. Morgenstern, *Adv. Pharmacol.* (1994) 19–35.
- [98] C. Andersson, F. Piemonte, E. Mosialou, R. Weinander, T.H. Sun, G. Lundqvist, A.E. Adang, R. Morgenstern, *Biochim. Biophys. Acta* 2 (1995) 277–283.
- [99] R. Svensson, J. Alander, R.N. Armstrong, R. Morgenstern, *Biochemistry* 27 (2004) 8869–8877.
- [100] R. Morgenstern, R. Svensson, B.A. Bernat, R.N. Armstrong, *Biochemistry* 11 (2001) 3378–3384.
- [101] I. Schmidt-Krey, K. Murata, T. Hirai, K. Mitsuoka, Y. Cheng, R. Morgenstern, Y. Fujiyoshi, H. Hebert, *J. Mol. Biol.* 2 (1999) 243–253.
- [102] I. Schmidt-Krey, K. Mitsuoka, T. Hirai, K. Murata, Y. Cheng, Y. Fujiyoshi, R. Morgenstern, H. Hebert, *EMBO J.* 23 (2000) 6311–6316.
- [103] P.J. Holm, R. Morgenstern, H. Hebert, *Biochim. Biophys. Acta* 2 (2002) 276–285.
- [104] P. Tito, E.J. Nettleton, C.V. Robinson, *J. Mol. Biol.* 2 (2000) 267–278.
- [105] A.J. Waring, P.W. Mobley, L.M. Gordon, *Proteins* (1998) 38–49.
- [106] M.Y. Kim, C.S. Maier, D.J. Reed, M.L. Deinzer, *J. Am. Chem. Soc.* 40 (2001) 9860–9866.
- [107] C. Hagman, P. Hakansson, J. Buijs, K. Hakansson, *J. Am. Soc. Mass Spectrom.* 5 (2004) 639–646.

- [108] F. Wang, W. Li, M.R. Emmett, C.L. Hendrickson, A.G. Marshall, Y.L. Zhang, L. Wu, Z.Y. Zhang, *Biochemistry* 44 (1998) 15289–15299.
- [109] X. Yan, D. Broderick, M.E. Leid, M.I. Schimerlik, M.L. Deinzer, *Biochemistry* 4 (2004) 909–917.
- [110] Z. Zhang, C.B. Post, D.L. Smith, *Biochemistry* 35 (1996) 779–791.
- [111] A. Nazabal, M. Laguerre, J.M. Schmitter, J. Vaillier, S. Chaignepain, J. Velours, *J. Am. Soc. Mass Spectrom.* 5 (2003) 471–481.
- [112] K. Dharmasiri, D.L. Smith, *Anal. Chem.* 14 (1996) 2340–2344.
- [113] V. Tsui, C. Garcia, S. Cavagnero, G. Siuzdak, H.J. Dyson, P.E. Wright, *Protein Sci.* 1 (1999) 45–49.
- [114] W.L. DeLano, *The PyMOL Molecular Graphics System*, DeLano Scientific, San Carlos, CA, 2002.
- [115] W. Bode, D. Turk, A. Karshikov, *Protein Sci.* 4 (1992) 426–471.